Pramana – J. Phys. (2022) 96:128
https://doi.org/10.1007/s12043-022-02359-2

A study on the dynamics of alkali–silica chemical reaction by using Caputo fractional derivative

PUSHPENDRA KUMAR[1],*, V GOVINDARAJ[1], VEDAT SUAT ERTURK[2] and MAGDA H ABDELLATTIF[3]

[1]Department of Mathematics, National Institute of Technology Puducherry, Karaikal 609 609, India
[2]Department of Mathematics, Faculty of Arts and Sciences, Ondokuz Mayis University, Atakum 55200, Samsun, Turkey
[3]Department of Chemistry, College of Science, Taif University, Al-Haweiah, P.O. Box 11099, Taif 21944, Saudi Arabia

*Corresponding author. kumarsaraswatpk@gmail.com

MS received 13 November 2021; revised 28 January 2022; accepted 1 February 2022

Abstract. In this paper, we propose a mathematical study to simulate the dynamics of alkali–silica reaction (ASR) by using the Caputo fractional derivative. We solve a non-linear fractional-order system containing six differential equations to understand the ASR. For proving the existence of a unique solution, we use some recent novel properties of Mittag–Leffler function along with the fixed point theory. The stability of the proposed system is also proved by using Ulam–Hyers technique. For deriving the fractional-order numerical solution, we use the well-known Adams–Bashforth–Moulton scheme along with its stability. Graphs are plotted to understand the given chemical reaction practically. The main reason to use the Caputo-type fractional model for solving the ASR system is to propose a novel mathematical formulation through which the ASR mechanism can be efficiently explored. This paper clearly shows the importance of fractional derivatives in the study of chemical reactions.

Keywords. Alkali–silica reaction; concrete; fractional-order mathematical model; Caputo fractional derivative; existence and uniqueness; Adams–Bashforth–Moulton scheme.

PACS Nos 82.40.Bj; 05.45.-a; 82.20.Wt; 02.60.Lj

1. Introduction

Concrete cancer, named as alkali–silica reaction (ASR), is an injurious protuberance reaction that comes over time in concrete between the paste of highly alkaline cement and the reactive amorphous silica presented in numerous usual aggregates, giving adequate moisture. This harmful chemical reaction is the reason for the elaboration of the exchanged aggregate by the fabrication of a viscous and soluble sodium silicate gel ($Na_2SiO_3{\cdot}nH_2O$, also indicated $Na_2H_2SiO_4{\cdot}nH_2O$). When this hygroscopic gel absorbs water, it swells and expands in volume: it applies a smashing stress inside the siliceous aggregate, and becomes the reason of death or loss of stability of the concrete, at the end leading to its failure. This chemical reaction induces grave cracking in concrete, causing structural losses and destruction of a specific structure (patterns can be seen from figure 1). For the first time, Thomas E Stanton in California with his research in 1940 [1], recognised the spreading of concrete via reaction between aggregates and cement.

ASR is a multistaged [2] complex [3] chemical reaction and virtually an acid–base reaction. In the pore solution, silica in solid form acts as an acid reactant, whereas sodium and/or potassium hydroxide, as well as may be calcium, are key reactants. Water is the medium of the reaction and calcium sodium silicate hydrate, or calcium potassium silicate hydrate [4] are the product of the reaction, based on the relative conjuncture of the cement paste and the age of the ASR gel that is produced [5]. Alkali aluminate, alkali sulphates and solid solution of belite are forms in which the alkalis are mixed in the Portland cement. Among these, alkali sulphates are the cardinal and water-soluble phase, that

Published online: 29 June 2022

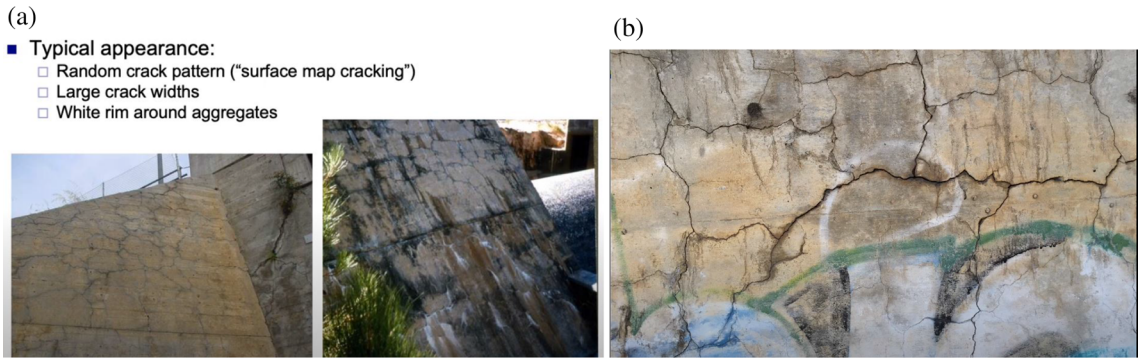

Figure 1. Patterns of alkali–silica reaction (ASR).

means in the pore solution, sulphate is the counter ion of the alkalis at the starting phase of cement hydration. In that manner, when ettringite's subsequent precipitation is finished then the alkalis' counter ion becomes hydroxide. It will play a role in the growth of the pH of the pore solution when both alkali ions (K^+ and Na^+) and hydroxide ions (OH^-) condense at a substantially high level to attack the reactive silica in the aggregate to build alkali–silica gel [6].

At the first phase, the reaction starts from the periphery of the aggregate without producing expansion. Then the expansion begins inboard the aggregate where alkali-rich ASR gel is enclosed within the microstructure of the reacted aggregate. In the next phase, concrete deterioration becomes much observable when the cement paste begins cracking, and diminution extends by enhancing the density and width of the cracks. In the end, severe damage occurs after active expansion of concrete, including structural failures. Larger aggregate leads to retaining larger concentrations of alkali ions and OH within the aggregate. So manufacturing of expansive alkali-type ASR gel starts inside the crude cluster, rather than on the layer where calcium from the paste of cement is administrated. It defines the grievous cracking tentative in the unrefined cluster and the earlier expiry of the reaction in the immaculate aggregate. When ASR gel transmigrates from the effective aggregate and accesses the paste of cement, it contends calcium and leaves alkali, thus its conformation influences one of the CSH gel and then squanders the power for diffusion, successively forwarding to termination of the ASR [7]. This compositional variation of ASR gel (the proportion of substitution of alkalis by calcium), that stows rifts from the reactive aggregate into the paste of cement, has also a 'sigmoidal curve' indicative of a diffusion mechanism [8]. For more studies on the given reaction, one can refer to the papers mentioned in the cited references.

In this paper, we are intended to study a mathematical model for understanding the mechanism of alkali–silica reaction by using one of the most famous Caputo fractional derivative. Nowadays, a number of real-world problems have been discussed by using fractional derivatives [9–13]. In the mathematical epidemiology, various types of fractional-order models have been proposed to simulate different types of diseases [14–17]. Particularly, the current deadly epidemic called Covid-19 was studied by using fractional-order models [18,19]. In [20], authors have studied the dynamics of cancer therapy by using the Caputo-type time-delay system. Kumar *et al* [21] have discussed a complex fractional-order model for describing the love story of a couple. Kumar *et al* [22] have explored the outbreaks of Covid-19 in Argentina by using the daily reported cases. Study given in [23] is dedicated to the Covid-19 forecasting in Cameroon by using Caputo fractional derivative. Kumar and Erturk [24] have proposed a new generalised Caputo-type mathematical model for studying an infection in the population of butterflies. In [25], a study on tuberculosis is proposed. In [26], dynamics of 2019-nCoV was defined in Spain along with optimal control problem. In [27], Covid-19 cases in Bangladesh and India were studied by using a novel fractional-order mathematical model. Abboubakar *et al* [28] have solved a model of malaria epidemic by using Euler and Adams–Bashforth methods. Kumar and Erturk [29] have solved a Covid-19 model by using a modified form of the well-known predictor–corrector method. Kumar *et al* [30] have proposed a new model of Covid-19 by taking the idea of vaccine rate. A mathematical model for lassa hemorrhagic fever is given in [31]. In [32], a study on CDV and rabies epidemics is proposed in the sense of fractional derivatives. A mathematical model for describing the dynamics of huanglongbing transmission in the population of citrus trees is given in ref. [33]. Study given in [34] discusses the mathematical structure of mosaic epidemic. A new, efficient and easy algorithm to solve the generalised Caputo-type fractional-order initial value problems is given in ref. [35]. Odibat *et al* [36] have proposed a modified form of the redictor–corrector (P–C) algorithm to simulate the time-delay

type initial value problems in the sense of generalised Caputo fractional derivative. In [37], one more generalised version of P–C algorithm is given. Angstmann *et al* [38] have proved the occurrence of intrinsic discontinuities in the solutions of Caputo–Fabrizio and Atangana–Baleanu-type evolution equations.

The current paper is arranged as follows: In §2, we recall some definitions and results. In §3, the fractional-order model dynamics is given in the sense of Caputo derivative. Analysis related to the existence of solution along with the derivation of numerical solution by using Adams–Bashforth–Moulton scheme is given in §4. Many experimental simulations are given in §5. At the end, we finish the paper with a conclusion.

2. Preliminaries

Firstly, we recall the following preliminaries:

DEFINITION 1

The Riemann–Liouville (RL) fractional-order integral of a function $G(t) \in C_\eta\ (\eta \geq -1)$ is given by [39]

$$J^\gamma G(t) = \frac{1}{\Gamma(\gamma)} \int_0^t (t-s)^{\gamma-1} G(s) \mathrm{d}s,$$
$$J^0 G(t) = G(t).$$

DEFINITION 2

The Caputo fractional derivative of order $\gamma > 0$ of the function $G : (0, \infty) \to \mathbb{R}$ is given by [39]

$$D_t^\gamma G(t) = \frac{1}{\Gamma(k-\gamma)} \int_0^t (t-\xi)^{k-\gamma-1} G^k(\xi) \mathrm{d}\xi, \quad (1)$$

where $k = [\gamma] + 1$ and $[\gamma]$ is the integer part of γ.

DEFINITION 3

The series expansion of the two-parametrised form of the Mittag–Leffler function for $a,\ b > 0$ is given by [40]

$$E_{a,\,b}(t) = \sum_{t=0}^{\infty} \frac{t^i}{\Gamma(ai+b)}. \quad (2)$$

Lemma 1. *Let* $d, e, l, h, r, \gamma > 0$. *Then there exists a real number* $\alpha > 0$ *such that for* $t \in [0, l]$,

$$t^h E_{d,e+\gamma}(\alpha t^d) < r E_{d,e}(\alpha t^d). \quad (3)$$

Proof. Refer to Lemma 2.1 in [40]. □

Theorem 1. *Let* $d, r, l, \gamma > 0$. *If* $e < \min\{\gamma, 1\}$, *then there exists a real number* $\alpha > 0$ *such that*

$$\frac{1}{\Gamma(\gamma)} \int_0^t (t-s)^{\gamma-1} \frac{E_{d,1-e}(\alpha s^d)}{s^e} \mathrm{d}s < r E_{d,\,1-e}(\alpha t^d),$$
$$t \in [0, l]. \quad (4)$$

Proof. Refer to Theorem 2.1 in [40]. □

3. Model dynamics

In this section, we model the chemical reactions which are given in ref. [6] [eqs (1)–(3)] by using Caputo fractional derivative operator. OH^- ions perform the hydrolysis of the reactive silica (siloxane) to prepare an alkali–silica gel. In that hydrolysis reaction, the high pH pore fluid reacts with Si–O–Si bonds to make silicic acid (silanol bond) and alkali silicate gel, as follows:

$$\underbrace{\overbrace{\mathrm{Si-O-Si}}^{\Lambda_1}}_{\text{Siloxane}} + \underbrace{\overbrace{\mathrm{R^+ + OH^-}}^{\Lambda_2}}_{\text{Hydroxyl ions}} \xrightarrow{\beta_1} \underbrace{\overbrace{\mathrm{Si-O-R}}^{\Lambda_3}}_{\text{Alkali-silicate (gel)}} + \underbrace{\overbrace{\mathrm{H-O-Si}}^{\Lambda_4}}_{\text{Silicic acid}}, \quad (5)$$

where R^+ denotes an alkali ion such as Na^+ or K^+.

The silicic acid which is formed here is weak, so that it instantly reacts with further hydroxyl releasing water and negative charged Si–O^-, thus readily copious and dapper potassium, calcium and sodium ions will protrude in the gel to equilibrate the species having negative charge.

$$\underbrace{\overbrace{\mathrm{H-O-Si}}^{\Lambda_4}}_{\text{Silicic acid}} + \underbrace{\overbrace{\mathrm{R^+ + OH^-}}^{\Lambda_2}}_{\text{Hydroxyl ions}} \xrightarrow{\beta_2} \underbrace{\overbrace{\mathrm{Si-O-R}}^{\Lambda_3}}_{\text{Alkali silicate (gel)}} + \underbrace{\overbrace{\mathrm{H_2O}}^{\Lambda_5}}_{\text{Water}}. \quad (6)$$

The resultant alkali silicate (alkali silicate gel) is hygroscopic (expands in the presence of water).

$$\underbrace{\overbrace{\mathrm{Si-O-R}}^{\Lambda_3}}_{\text{Alkali-silicate (gel)}} + \underbrace{\overbrace{\mathrm{nH_2O}}^{\Lambda_5}}_{\text{Water}} \xrightarrow{\beta_3} \underbrace{\overbrace{\mathrm{Si-O^- + (H_2O)_n + Na^+}}^{\Lambda_6}}_{\text{Expanded alkali silicate (gel)}}. \quad (7)$$

In eqs (5)–(7), $\beta_1,\ \beta_2,\ \beta_3$ are the reaction rates. So, the rate of change of concentration for all the six given constituents $\Lambda_1,\ \Lambda_2,\ \Lambda_3,\ \Lambda_4,\ \Lambda_5,\ \Lambda_6$ in the sense of Caputo fractional derivative can be expressed as follows:

$$\begin{cases} {}^{\gamma}D_t^C \Lambda_1(t) &= -\beta_1^{\gamma}\Lambda_1(t)\Lambda_2(t), \\ {}^{\gamma}D_t^C \Lambda_2(t) &= -\beta_1^{\gamma}\Lambda_1(t)\Lambda_2(t) - \beta_2^{\gamma}\Lambda_4(t)\Lambda_2(t), \\ {}^{\gamma}D_t^C \Lambda_3(t) &= \beta_1^{\gamma}\Lambda_1(t)\Lambda_2(t) + \beta_2^{\gamma}\Lambda_4(t)\Lambda_2(t) \\ & \quad -\beta_3^{\gamma}\Lambda_3(t)\Lambda_5(t), \\ {}^{\gamma}D_t^C \Lambda_4(t) &= \beta_1^{\gamma}\Lambda_1(t)\Lambda_2(t) - \beta_2^{\gamma}\Lambda_4(t)\Lambda_2(t), \\ {}^{\gamma}D_t^C \Lambda_5(t) &= \beta_2^{\gamma}\Lambda_4(t)\Lambda_2(t) - \beta_3^{\gamma}\Lambda_3(t)\Lambda_5(t), \\ {}^{\gamma}D_t^C \Lambda_6(t) &= \beta_3^{\gamma}\Lambda_3(t)\Lambda_5(t), \end{cases} \tag{8}$$

where ${}^{\gamma}D_t^C$ is the Caputo-type fractional operator of order γ. We use fractional order power γ on both sides in the above model for taking the equal dimension time$^{-\gamma}$. The advantage to use this Caputo operator is that the given operator can be easily generalised as an integer-order derivative if fractional-order γ tends to one. Also, efficiency of capturing memory effects increases the impact of fractional derivatives which is the main motivation of this new fractional-order model. To our knowledge, the given chemical reaction is not yet studied by any kind of fractional derivatives which increases the impact of this model.

Now for further analysing the existence of solution and numerical approximations of fractional-order system (8), we re-write it to a compact equivalent form with the help of singular kernels, which is as follows:

$$\begin{cases} {}^{\gamma}D_t^C \Lambda_1(t) = \mathcal{K}_1(t, \Lambda_1), \\ {}^{\gamma}D_t^C \Lambda_2(t) = \mathcal{K}_2(t, \Lambda_2), \\ {}^{\gamma}D_t^C \Lambda_3(t) = \mathcal{K}_3(t, \Lambda_3), \\ {}^{\gamma}D_t^C \Lambda_4(t) = \mathcal{K}_4(t, \Lambda_4), \\ {}^{\gamma}D_t^C \Lambda_5(t) = \mathcal{K}_5(t, \Lambda_5), \\ {}^{\gamma}D_t^C \Lambda_6(t) = \mathcal{K}_6(t, \Lambda_6), \end{cases} \tag{9}$$

with initial conditions $\Lambda_1(0) = \Lambda_{1_0}$, $\Lambda_2(0) = \Lambda_{2_0}$, $\Lambda_3(0) = \Lambda_{3_0}$, $\Lambda_4(0) = \Lambda_{4_0}$, $\Lambda_5(0) = \Lambda_{5_0}$, $\Lambda_6(0) = \Lambda_{6_0}$. Here $\mathcal{K}_1$, $\mathcal{K}_2$, $\mathcal{K}_3$, $\mathcal{K}_4$, $\mathcal{K}_5$ and $\mathcal{K}_6$ are the proposed singular kernels with respect to the given classes.

4. Fractional-order analysis of the proposed model

In this section, we analyse the existence of a unique global solution using the properties of Schauder fixed-point theorem and Mittag–Leffler function using important lemmas and theorems. After that, we shall derive the numerical solution of the model with the help of a numerical scheme.

4.1 *Analysis of the existence and uniqueness*

In this section, we adopt the first equation of the compact form (9) and perform the necessary analysis (for other equations, the analysis will be the same). It is well known that the first equation of the initial value problem (9) of Caputo-type is equivalent to the Volterra integral equation

$$\Lambda_1(t) = \Lambda_1(0) + \frac{1}{\Gamma(\gamma)}\int_0^t (t-s)^{\gamma-1}\mathcal{K}_1(s, \Lambda_1)\mathrm{d}s, \tag{10}$$

with the assumption of continuity of Λ_1. In a most familiar way, we convert the given integral eq. (10) with the fixed-point problem by using $\mathcal{O}$ written by

$$\mathcal{O}\Lambda_1(t) = \Lambda_1(0) + \frac{1}{\Gamma(\gamma)}\int_0^t (t-s)^{\gamma-1}\mathcal{K}_1(s, \Lambda_1)\mathrm{d}s. \tag{11}$$

Let $L > 0$ and Y be a Banach space consisting of function $\Lambda_1 \in C[0, L]$ associated with the Chebyshev-type norm $\|\cdot\|$.

Lemma 2. *Assume that B is a bounded, closed and convex subset of Banach space Y and $\mathcal{O}(B) \subset B$, then $\mathcal{O}$ exists at least one fixed point inside B.*

Proof. With the application of Schauder's fixed-point theorem, this result can be easily proved. For complete justification of the proof, refer to Theorem 6.1 in ref. [41]. □

Now, by using Lemma 2, initial value problem (IVP) (9) is converted to the problem for simulating a bounded, closed and convex subset of space Y with the condition $\mathcal{O}(B) \subset B$.

For defining the upcoming result, we fix the assumptions given below:

($\mathcal{A}_1$) $\mathcal{K}_1 : [0, T] \times R \to R$ is continuous.

($\mathcal{A}_2$) Constants $T_1 \in (0, T]$, $a \in [0, \min\{\gamma, 1\})$, p_1, $p_2 \in (0, 1]$, b_0, b_1, b_2, $b_3 > 0$ exist, such that

$$|\mathcal{K}_1(t, x)| \leq \begin{cases} b_0 + \dfrac{b_1}{t^a}|x|^{p_1} \text{ for } t \in (0, T_1] \text{ and } x \in R \\ b_2 + b_3|x|^{p_2} \text{ for } t \in [T_1, T] \text{ and } x \in R. \end{cases} \tag{12}$$

Theorem 2. *Assume that ($\mathcal{A}_1$) and ($\mathcal{A}_2$) exist. Then IVP (9) has at least one solution in $C[0, T]$.*

Proof. Adopt a real number $0 \le r$ with $2rb_1 < 1$. From Theorem 1, a real number $\lambda_1 > 0$ exists such that

$$\frac{1}{\Gamma(\gamma)}\int_0^t (t-s)^{\gamma-1}\frac{E_{2,1-\gamma}(\lambda_1 s^2)}{s^\gamma}\mathrm{d}s < rE_{2,1-\gamma}(\lambda_1 t^2). \tag{13}$$

Take a real number $\lambda_2 > 0$ with $2b_3 < \lambda_2$. Derive a subset B of space Y in the form:

$$B = \{\Lambda_1 \in Y : |S(t)| \le \begin{Bmatrix} 2M_1E_{2,1-a}(\lambda_1 t^2) \text{ for } t \in [0, T_1] \\ 2M_2E_{\gamma,1}(\lambda_2 t^\gamma) \quad \text{for } t \in [T_1, T] \end{Bmatrix},$$

where

$$M_1 = \max\{\Gamma(1-a), \Gamma(1-a) \times \left[\Lambda_1(0) + \frac{b_0 T_1^\gamma}{\Gamma(\gamma+1)}\right]\}$$

and

$$M_2 = \max\left\{1, \Lambda_1(0) + 2M_1E_{2,1-\gamma}(\lambda_1 T_1^2) + \frac{b_2 T^\gamma}{\Gamma(\gamma+1)}\right\}.$$

It is convenient to show that B is bounded, closed and convex. By $(\mathcal{A}_2)$ and (13), we can see that for each $\Lambda_1 \in B$ and $t \in [0, T_1]$,

$$\begin{aligned}
|\mathcal{O}\Lambda_1(t)| &\le \Lambda_1(0) + \frac{1}{\Gamma(\gamma)}\int_0^t (t-s)^{\gamma-1} \times |\mathcal{K}_1(s, \Lambda_1(s))|\mathrm{d}s \\
&\le \Lambda_1(0) + \frac{1}{\Gamma(\gamma)}\int_0^t (t-s)^{\gamma-1} \times \left(b_0 + \frac{b_1}{s^\gamma}|\Lambda_1(s)|^{p_1}\right)\mathrm{d}s \\
&\le \Lambda_1(0) + \frac{b_0 t^\gamma}{\Gamma(\gamma+1)} + \frac{1}{\Gamma(\gamma)}\int_0^t (t-s)^{\gamma-1} \times \frac{b_1}{s^\gamma}|\Lambda_1(s)|^{p_1}\mathrm{d}s \le \Lambda_1(0) + \frac{b_0 t^\gamma}{\Gamma(\gamma+1)} \\
&\quad + \frac{b_1}{\Gamma(\gamma)}\int_0^t (t-s)^{\gamma-1} \times \frac{2M_1E_{2,1-\gamma}(\lambda_1 s^\beta)}{s^\gamma}\mathrm{d}s \\
&< M_1E_{2,1-\gamma}(\lambda_1 t^2) + 2rb_1M_1E_{2,1-\gamma}(\lambda_1 t^2) \\
&< 2M_1E_{2,1-\gamma}(\lambda_1 t^2).
\end{aligned}$$

From Theorem 10.1 in [42], we can say that for each $\Lambda_1 \in B$ and $t \in [T_1, T]$,

$$\begin{aligned}
|\mathcal{O}\Lambda_1(t)| &\le \Lambda_1(0) + \frac{1}{\Gamma(\gamma)}\int_0^{T_1} (t-s)^{\gamma-1} \times |\mathcal{K}_1(s, \Lambda_1(s))|\mathrm{d}s \\
&\quad + \frac{1}{\Gamma(\gamma)}\int_{T_1}^t (t-s)^{\gamma-1}|\mathcal{K}_1(s, u(s))|\mathrm{d}s \\
&\le \Lambda_1(0) + 2M_1E_{2,1-\gamma}(\lambda_1 T_1^2) \\
&\quad + \frac{1}{\Gamma(\gamma)}\int_0^t (t-s)^{\gamma-1}\left(b_2 + b_3|\Lambda_1(s)|^{p2}\right)\mathrm{d}s \\
&\le \Lambda_1(0) + 2M_1E_{2,1-\gamma}(\lambda_1 T_1^2) + \frac{b_2 t^\gamma}{\Gamma(\gamma+1)} \\
&\quad + \frac{1}{\Gamma(\gamma)}\int_0^t (t-s)^{\gamma-1}2b_3M_2E_{\gamma,1}(\lambda_2 s^\gamma)\mathrm{d}s \\
&< M_2 + \frac{2b_3}{\lambda_2}M_2E_{\gamma,1}(\lambda_2 t^\gamma) < 2M_2E_{\gamma,1}(\lambda_2 t^\gamma)
\end{aligned}$$

which gives $T : B \to B$. Using Lemma 2, IVP (9) has at least one solution in B. □

Now, for proving the uniqueness of the solution, we take the following assumption:

$(\mathcal{A}_3)$ There exist constants $a \in [0, \min\{\gamma, 1\})$, b_1, $b_2 > 0$, $T_1 \in (0, T]$ such that

$$|\mathcal{K}_1(t, \Lambda_1^*) - \mathcal{K}_1(t, \Lambda_1^{**})| \le \begin{cases} \frac{b_1}{t^a}|\Lambda_1^* - \Lambda_1^{**}| & \text{for } t \in (0, T_1] \text{ and } \Lambda_1^*, \Lambda_1^{**} \in R \\ b_2|\Lambda_1^* - \Lambda_1^{**}| & \text{for } t \in [T_1, T] \text{ and } \Lambda_1^*, \Lambda_1^{**} \in R. \end{cases} \tag{14}$$

Theorem 3. *Assume that* $(\mathcal{A}_1)$ *and* $(\mathcal{A}_3)$ *hold. Then IVP* (9) *has a unique solution in the space* $C[0, T]$.

Proof. By $(\mathcal{A}_3)$, it is convenient to show that $(\mathcal{A}_2)$ exists. From Theorem 2, model (9) has at least one solution. Assume that system (9) has two different solutions. Then it is obvious to say that the integral equation (10) will also have two solutions such as Λ_1 and Λ_1^* where $\|\Lambda_1 - \Lambda_1^*\| > 0$. Take a real number $r > 0$ with $rb < 1$.

So, from Theorem 1, a real number $\lambda > 0$ exists such that

$$\frac{1}{\Gamma(\gamma)}\int_0^t (t-s)^{\gamma-1}\frac{E_{2,1-\gamma}(\lambda_1 s^2)}{s^\gamma}\mathrm{d}s < rE_{2,1-\gamma}(\lambda_1 t^2), \ t \in [0, T_1]. \tag{15}$$

Derive U and V as follows:

$$\begin{aligned}
U &= \inf\{m : |\Lambda_1(t) - \Lambda_1^*(t)| \le mE_{2,1-\gamma}(\lambda t^2), t \in [0, T_1]\}, \\
V &= \inf\{t \in [0, T_1] : |\Lambda_1(t) - \Lambda_1^*(t)| = UE_{2,1-\gamma}(\lambda t^2)\}.
\end{aligned}$$

If $U \neq 0$, then it is clear that $V \neq 0$. Using $(\mathcal{A}_3)$ and (15), we get

$$\begin{aligned} UE_{2,1-\gamma}(\lambda V^2) &= |\Lambda_1(V) - \Lambda_1^*(V)| \\ &\leq \frac{1}{\Gamma(\gamma)} \int_0^V (V-s)^{\gamma-1} |\mathcal{K}_1(s, \Lambda_1(s)) \\ &\quad -\mathcal{K}_1(s, \Lambda_1^*(s))| \mathrm{d}s \\ &\leq \frac{1}{\Gamma(\gamma)} \int_0^V (V-s)^{\gamma-1} \frac{b}{s^\gamma} |\Lambda_1(s) \\ &\quad -\Lambda_1^*(s)| \mathrm{d}s \\ &\leq \frac{1}{\Gamma(\gamma)} \int_0^V (V-s)^{\gamma-1} \\ &\quad \frac{bME_{2,1-\gamma}(\lambda s^2)}{s^\gamma} \mathrm{d}s \\ &< rbME_{2,1-\gamma}(\lambda V^2) \\ &< ME_{2,1-\gamma}(\lambda V^2). \end{aligned}$$

That is not possible.

When $U = 0$, it is apparent that $\Lambda_1(t) = \Lambda_1^*(t), t \in [0, T_1]$. Take a real number $\lambda_1 > 0$ with $b_2 < \lambda_1$. Define U_1 and V_1 as follows:

$$\begin{aligned} U_1 &= \inf\{m : |\Lambda_1(t) - \Lambda_1^*(t)| \\ &\quad \leq mE_{\gamma,1}(\lambda_1 t^\gamma), t \in [T_1, T]\}, \\ V_1 &= \inf\{t \in [T_1, T] : |\Lambda_1(t) - \Lambda_1^*(t)| \\ &\quad = UE_{\gamma,1}(\gamma_1 t^\gamma)\}. \end{aligned}$$

We can see that $U_1 \neq 0$ and $V_1 \neq 0$. By $(\mathcal{A}_3)$ and Theorem 10.1 in [42], we have

$$\begin{aligned} &U_1 E_{\gamma,1}(\lambda_1 V_1^\gamma) \\ &= |\Lambda_1(V_1) - \Lambda_1^*(V_1)| \\ &\leq \frac{1}{\Gamma(\gamma)} \int_0^{V_1} (V_1 - s)^{\gamma-1} |\mathcal{K}_1(s, \Lambda_1(s)) \\ &\quad -\mathcal{K}_1(s, \Lambda_1^*(s))| \mathrm{d}s \\ &\leq \frac{1}{\Gamma(\gamma)} \int_T^{V_1} (V_1 - s)^{\gamma-1} b_2 |\Lambda_1(s) - \Lambda_1^*(s)| \mathrm{d}s \\ &\leq \frac{1}{\Gamma(\gamma)} \int_0^{V_1} (V_1 - s)^{\gamma-1} b_2 U_1 E_{\gamma,1}(\lambda_1 s^\gamma) \mathrm{d}s \\ &= \frac{b_2}{\lambda_1} U_1 E_{\gamma,1}(\lambda_1 V_1^\gamma) < U_1 E_{\gamma,1}(\lambda_1 V_1^\gamma). \end{aligned}$$

This is impossible. Thus, model (9) has a unique solution. □

4.2 *Stability of the model*

Theorem 4. [43] *Consider a metric space (F, R) which is completely generalised. Assume $A : F \to F$ is a strictly contractive operator. If there exists an integer $v \geq 0$ with $R(A^{v+1}d, A^v d) < \infty$ for some $d \in F$,*

(a) $\lim_{l \to +\infty} A^l d = d^*$ *is the unique fixed point of A in*

$$F^* := \left\{ d_1 \in F : R(A^v d, d_1) < \infty \right\}. \tag{16}$$

(b) *If $d_1 \in F^*$, then $R(d_1, d^*) \leq (1/(1-K))R(Ad_1, d_1)$.*
Here we are taking the space $X := C(I, \mathbb{R})$, where $I := [0, T]$.

Theorem 5. *Let $\mathcal{K}_1 : I \times \mathbb{R} \to \mathbb{R}$ is a continuous function and satisfies*

$$|\mathcal{K}_1(t, \Lambda_1^*) - \mathcal{K}_1(t, \Lambda_1^{**})| \leq L_p |\Lambda_1^* - \Lambda_1^{**}| \tag{17}$$

for all $t \in I$, $\Lambda_1^*, \Lambda_1^{**} \in \mathbb{R}$, and for some $L_p > 0$. If the absolutely continuous function $\Lambda_1 : I \to \mathbb{R}$ satisfies

$$\left| {}^C D_{0,t}^\gamma \Lambda_1(t) - \mathcal{K}_1(t, \Lambda_1(t)) \right| \leq \epsilon(t), \tag{18}$$

$\forall\ t \in I$, where $\epsilon > 0$ and $\rho(t)$ is a positive, non-decreasing and continuous function, then there is a solution Λ_1^* of first equation of model (9) such that

$$\begin{aligned} \left| \Lambda_1(t) - \Lambda_1^*(t) \right| &\leq \left(\frac{L_p + \delta}{\delta} \right) \\ &\quad \times \frac{M\mathbb{E}_\gamma\left((L_p + \delta)T^\gamma\right)}{\Gamma(\gamma+1)}, \epsilon\rho(t), \end{aligned} \tag{19}$$

where

$$M = \sup_{s \in [0,T]} \left(\frac{(s)^\gamma}{\mathbb{E}_\gamma\left((L_p + \delta)(s)^\gamma\right)} \right) \tag{20}$$

and δ is any positive constant.

Proof. Firstly, we derive the metric d on space X as follows:

$$\begin{aligned} d(\Lambda_1^*, \Lambda_1^{**}) = \inf \Bigg\{ D \in [0, \infty] : \frac{|\Lambda_1^*(t) - \Lambda_1^{**}(t)|}{\mathbb{E}_\gamma\left((L_p + \delta)(t)^\gamma\right)} \\ \leq D\rho(t), \forall\ t \in I \Bigg\}. \end{aligned} \tag{21}$$

Now, specify an operator $\mathcal{A} : X \to X$ such that

$$\begin{aligned} (\mathcal{A}\Lambda_1)(t) &:= \Lambda_1(0) + \frac{1}{\Gamma(\gamma)} \int_0^t (t-s)^{\gamma-1} \\ &\quad \times \mathcal{K}_1(s, \Lambda_1(s)) \mathrm{d}s. \end{aligned} \tag{22}$$

It is simple to write that $d(\mathcal{A}\Lambda_{1_0}, \Lambda_{1_0}) < \infty$, and $\{\Lambda_1 \in X : d(\Lambda_{1_0}, \Lambda_1) < \infty\} = X,\ \forall\ \Lambda_{1_0} \in X$.

First we show that the operator $\mathcal{A}$ is a strictly contractive operator by

$$|(\mathcal{A}\Lambda_1^*)(t) - (\mathcal{A}\Lambda_1^{**})(t)|$$

$$
\begin{aligned}
&\leq \left| \int_0^t \frac{(t-\xi)^{\gamma-1}}{\Gamma(\gamma)} \{\mathcal{K}_1(\xi, \Lambda_1^*(\xi)) \right. \\
&\quad \left. -\mathcal{K}_1(\xi, \Lambda_1^{**}(\xi))\} \mathrm{d}\xi \right| \\
&\leq \frac{1}{\Gamma(\gamma)} \int_0^t (t-\xi)^{\gamma-1} |\mathcal{K}_1(\xi, \Lambda_1^*(\xi)) \\
&\quad -\mathcal{K}_1(\xi, \Lambda_1^{**}(\xi))| \mathrm{d}\xi \\
&\leq L_p \int_0^t (t-\xi)^{\gamma-1} \frac{|\Lambda_1^*(\xi) - \Lambda_1^{**}(\xi)|}{\Gamma(\gamma)} \mathrm{d}\xi \\
&\leq \frac{L_p}{\Gamma(\gamma)} \int_0^t (t-\xi)^{\gamma-1} \frac{|\Lambda_1^*(\xi) - \Lambda_1^{**}(\xi)|}{\mathbb{E}_\gamma\big((L_p+\delta)(\xi)^\gamma\big)} \mathbb{E}_\gamma \\
&\quad \times \big((L_p+\delta)(\xi)^\gamma\big) \mathrm{d}\xi \\
&\leq \frac{L_p d(\Lambda_1^*, \Lambda_1^{**})}{\Gamma(\gamma)} \int_0^t (t-\xi)^{\gamma-1} \rho(\xi) \mathbb{E}_\gamma \\
&\quad \times \big((L_p+\delta)(\xi)^\gamma\big) \mathrm{d}\xi, \text{ for all } t \in I. \qquad (23)
\end{aligned}
$$

As ρ is non-decreasing,

$$
\begin{aligned}
&|(\mathcal{A}\Lambda_1^*)(t) - (\mathcal{A}\Lambda_1^{**})(t)| \\
&\leq \frac{L_p d(\Lambda_1^*, \Lambda_1^{**})}{\Gamma(\gamma)} \rho(t) \\
&\quad \times \int_0^t (t-\xi)^{\gamma-1} \mathbb{E}_\gamma\big((L_p+\delta)(\xi)^\gamma\big) \mathrm{d}\xi \\
&\leq \frac{L_p d(\Lambda_1^*, \Lambda_1^{**})}{L_p+\delta} \left(\mathbb{E}_\gamma\big((L_p+\delta)(\xi)^\gamma\big) - 1\right) \rho(t) \\
&\leq \frac{L_p d(\Lambda_1^*, \Lambda_1^{**})}{L_p+\delta} \left(\mathbb{E}_\gamma\big((L_p+\delta)(\xi)^\gamma\big)\right) \rho(t), \\
&\quad \text{for all } t \in I \qquad (24)
\end{aligned}
$$

so that

$$
d(\mathcal{A}\Lambda_1^*, \mathcal{A}\Lambda_1^{**}) \leq \frac{L_p}{L_p+\delta} d(\Lambda_1^*, \Lambda_1^{**})
$$

which shows that the operator $\mathcal{A}$ is a strictly contractive operator. Now, since we have

$$
\left| {}^C D_{0,t}^\gamma \Lambda_1(t) - \mathcal{K}_1(t, \Lambda_1(t)) \right| \leq \epsilon\rho(t) \qquad (25)
$$

then

$$
\begin{aligned}
&|\Lambda_1(t) - \mathcal{A}\Lambda_1(t), \Lambda_1(t))| \\
&\quad \leq \frac{\epsilon}{\Gamma(\gamma)} \rho(t) \int_0^t (t-\xi)^{\gamma-1} \rho(\xi) \mathrm{d}\xi \qquad (26)
\end{aligned}
$$

which implies that

$$
\begin{aligned}
&\frac{|\Lambda_1(t) - \mathcal{A}\Lambda_1(t), \Lambda_1(t))|}{\mathbb{E}_\gamma\big((L_p+\delta)(\xi)^\gamma\big)} \\
&\leq \frac{\epsilon}{\Gamma(\gamma+1)} \rho(t) \frac{(t-\xi)^\gamma}{\mathbb{E}_\gamma\big((L_p+\delta)(\xi)^\gamma\big)} \\
&\leq \frac{\epsilon M}{\Gamma(\gamma+1)} \rho(t). \qquad (27)
\end{aligned}
$$

Therefore,

$$
d(\Lambda_1, \mathcal{A}\Lambda_1) \leq \epsilon \frac{M}{\Gamma(\gamma+1)}.
$$

By using Theorem 4, there is a solution Λ_1^* of the first equation of (9) such that

$$
d(\Lambda_1, \Lambda_1^*) \leq \epsilon \left(\frac{L_p+\delta}{\delta}\right) \frac{M}{\Gamma(\gamma+1)}
$$

so that,

$$
\begin{aligned}
|\Lambda_1(t) - \Lambda_1^*(t)| &\leq \left(\frac{L_p+\delta}{\delta}\right) \frac{M\mathbb{E}_\gamma\big((L_p+\delta)T^\gamma\big)}{\Gamma(\gamma+1)}, \\
&\quad \epsilon\rho(t) \text{ for all } t \in [0, T]. \qquad \square
\end{aligned}
$$

4.3 *Numerical solution of the given model by using Adams–Bashforth–Moulton (ABM) method*

We know that generally in the case of fractional-order mathematical models, deriving the exact solution is not possible. In these cases, probably we use numerical methods to find the approximate solutions. For the last few years, there is a very high demand of various types of approximation methods to simulate different fractional-order systems. Some very recent numerical schemes can be seen in refs [35–37]. In that way, for solving the proposed Caputo-type fractional model (9), we use the very well-known Adams–Bashforth–Moulton scheme. To write the numerical solution by using this scheme, we just consider the first differential equation of the model (9):

$$
\begin{cases}
{}^\gamma D_t^C \Lambda_1(t) = \mathcal{K}_1(t, \Lambda_1), \quad 0 \leq t \leq T, \\
\Lambda_1(0) = \Lambda_{1_0}, \quad k = 0, 1, 2, \ldots, m-1, \text{ where } m = [\gamma].
\end{cases} \qquad (28)
$$

This related Volterra integral equation is given by

$$
\Lambda_1(t) = \Lambda_1(0) + \frac{1}{\Gamma(\gamma)} \int_0^t (t-s)^{\gamma-1} \mathcal{K}_1(s, \Lambda_1) \mathrm{d}s. \qquad (29)
$$

Then, by following the method used in ref. [23], and taking $\gamma \in [0, 1]$, $0 \leq t \leq T$, $h = T/N$ and $t_n = nh$, for $n = 0, 1, 2, \ldots, N \in Z^+$, the solution of the given model (9) or the numerical solution of the proposed model (8) is written as

$$
\Lambda_{1_{n+1}} = \Lambda_{1_0} + \frac{h^\gamma}{\Gamma(\gamma+2)} \big(- \beta_1^\gamma \Lambda_{1_{n+1}}^P(t) \Lambda_{2_{n+1}}^P(t) \big)
$$

$$
\begin{aligned}
&+\frac{h^\gamma}{\Gamma(\gamma+2)}\sum_{j=0}^{n} a_{j,n+1}\big(-\beta_1^\gamma \Lambda_{1_j}(t)\Lambda_{2_j}(t)\big),\\
\Lambda_{2_{n+1}} &= \Lambda_{2_0}+\frac{h^\gamma}{\Gamma(\gamma+2)}\big(-\beta_1^\gamma \Lambda^P_{1_{n+1}}(t)\Lambda^P_{2_{n+1}}(t)\\
&-\beta_2^\gamma \Lambda^P_{4_{n+1}}(t)\Lambda^P_{2_{n+1}}(t)\big)\\
&+\frac{h^\gamma}{\Gamma(\gamma+2)}\sum_{j=0}^{n} a_{j,n+1}\big(-\beta_1^\gamma \Lambda_{1_j}(t)\Lambda_{2_j}(t)\\
&-\beta_2^\gamma \Lambda_{4_j}(t)\Lambda_{2_j}(t)\big),\\
\Lambda_{3_{n+1}} &= \Lambda_{3_0}+\frac{h^\gamma}{\Gamma(\gamma+2)}\big(\beta_1^\gamma \Lambda^P_{1_{n+1}}(t)\Lambda^P_{2_{n+1}}(t)\\
&+\beta_2^\gamma \Lambda^P_{4_{n+1}}(t)\Lambda^P_{2_{n+1}}(t)\\
&-\beta_3^\gamma \Lambda^P_{3_{n+1}}(t)\Lambda^P_{5_{n+1}}(t)\big)\\
&+\frac{h^\gamma}{\Gamma(\gamma+2)}\sum_{j=0}^{n} a_{j,n+1}\big(\beta_1^\gamma \Lambda_{1_j}(t)\Lambda_{2_j}(t)\\
&+\beta_2^\gamma \Lambda_{4_j}(t)\Lambda_{2_j}(t)\\
&-\beta_3^\gamma \Lambda_{3_j}(t)\Lambda_{5_j}(t)\big),\\
\Lambda_{4_{n+1}} &= \Lambda_{4_0}+\frac{h^\gamma}{\Gamma(\gamma+2)}\big(\beta_1^\gamma \Lambda^P_{1_{n+1}}(t)\Lambda^P_{2_{n+1}}(t)\\
&-\beta_2^\gamma \Lambda^P_{4_{n+1}}(t)\Lambda^P_{2_{n+1}}(t)\big)\\
&+\frac{h^\gamma}{\Gamma(\gamma+2)}\sum_{j=0}^{n} a_{j,n+1}\big(\beta_1^\gamma \Lambda_{1_j}(t)\Lambda_{2_j}(t)\\
&-\beta_2^\gamma \Lambda_{4_j}(t)\Lambda_{2_j}(t)\big),\\
\Lambda_{5_{n+1}} &= \Lambda_{5_0}+\frac{h^\gamma}{\Gamma(\gamma+2)}\big(\beta_2^\gamma \Lambda^P_{4_{n+1}}(t)\Lambda^P_{2_{n+1}}(t)\\
&-\beta_3^\gamma \Lambda^P_{3_{n+1}}(t)\Lambda^P_{5_{n+1}}(t)\big)\\
&+\frac{h^\gamma}{\Gamma(\gamma+2)}\sum_{j=0}^{n} a_{j,n+1}\big(\beta_2^\gamma \Lambda_{4_j}(t)\Lambda_{2_j}(t)\\
&-\beta_3^\gamma \Lambda_{3_j}(t)\Lambda_{5_j}(t)\big),\\
\Lambda_{6_{n+1}} &= \Lambda_{6_0}+\frac{h^\gamma}{\Gamma(\gamma+2)}\big(\beta_3^\gamma \Lambda^P_{3_{n+1}}(t)\Lambda^P_{5_{n+1}}(t)\big)\\
&+\frac{h^\gamma}{\Gamma(\gamma+2)}\sum_{j=0}^{n} a_{j,n+1}\big(\beta_3^\gamma \Lambda_{3_j}(t)\Lambda_{5_j}(t)\big),
\end{aligned}
\tag{30}
$$

where

$$
\begin{aligned}
\Lambda^P_{1_{n+1}} &= \Lambda_{1_0}+\frac{1}{\Gamma(\gamma)}\sum_{j=0}^{n} b_{j,n+1}\big(-\beta_1^\gamma \Lambda_{1_j}(t)\Lambda_{2_j}(t)\big),\\
\Lambda^P_{2_{n+1}} &= \Lambda_{2_0}+\frac{1}{\Gamma(\gamma)}\sum_{j=0}^{n} b_{j,n+1}\big(-\beta_1^\gamma \Lambda_{1_j}(t)\Lambda_{2_j}(t)\\
&-\beta_2^\gamma \Lambda_{4_j}(t)\Lambda_{2_j}(t)\big),\\
\Lambda^P_{3_{n+1}} &= \Lambda_{3_0}+\frac{1}{\Gamma(\gamma)}\sum_{j=0}^{n} b_{j,n+1}\big(\beta_1^\gamma \Lambda_{1_j}(t)\Lambda_{2_j}(t)\\
&+\beta_2^\gamma \Lambda_{4_j}(t)\Lambda_{2_j}(t)-\beta_3^\gamma \Lambda_{3_j}(t)\Lambda_{5_j}(t)\big),\\
\Lambda^P_{4_{n+1}} &= \Lambda_{4_0}+\frac{1}{\Gamma(\gamma)}\sum_{j=0}^{n} b_{j,n+1}\big(\beta_1^\gamma \Lambda_{1_j}(t)\Lambda_{2_j}(t)\\
&-\beta_2^\gamma \Lambda_{4_j}(t)\Lambda_{2_j}(t)\big),\\
\Lambda^P_{5_{n+1}} &= \Lambda_{5_0}+\frac{1}{\Gamma(\gamma)}\sum_{j=0}^{n} b_{j,n+1}\big(\beta_2^\gamma \Lambda_{4_j}(t)\Lambda_{2_j}(t)\\
&-\beta_3^\gamma \Lambda_{3_j}(t)\Lambda_{5_j}(t)\big),\\
\Lambda^P_{6_{n+1}} &= \Lambda_{6_0}+\frac{1}{\Gamma(\gamma)}\sum_{j=0}^{n} b_{j,n+1}\big(\beta_3^\gamma \Lambda_{3_j}(t)\Lambda_{5_j}(t)\big)
\end{aligned}
\tag{31}
$$

and

$$
a_{j,n+1}=\begin{cases} n^{\gamma+1}-(n-\gamma)(1+n), & j=0,\\ (n+2-j)^{\gamma+1}-2(n+1-j)^{\gamma+1}\\ \quad +(n-j)^{\gamma+1}, & 1\le j\le n,\\ 1, & j=n+1,\end{cases}
$$

$$
b_{j,n+1}=\frac{h^\gamma}{\gamma}\big((n+1-j)^\gamma-(n-j)^\gamma\big),\quad 0\le j\le n.
$$

4.3.1 *Stability analysis.*

Lemma 3. [44] *If* $0<\gamma<1$ *and* r *is a non-negative integer, then there exists the positive constants* $C_{\gamma,1}$ *and* $C_{\gamma,2}$ *which depend on* γ, *such that*

$$
(1+r)^\gamma-r^\gamma\le C_{\gamma,1}(1+r)^{\gamma-1}
$$

and

$$
(r+2)^{\gamma+1}-2(r+1)^{\gamma+1}+r^{\gamma+1}\le C_{\gamma,2}(r+1)^{\gamma-1}.
$$

Lemma 4. [44] *Let* $d_{p,n}=(n-p)^{\gamma-1}(p=1,2,\ldots,n-1)$ *and* $d_{p,n}=0$ *for* $p\ge n$, $\gamma, h, M, T>0$, $rh\le T$ *and* r *is a positive integer. Let* $\sum_{p=r}^{p=n} d_{p,n}|e_p|=0$ *for* $k>n\ge 1$. *If*

$$
|e_n|\le Mh^\gamma\sum_{p=1}^{n-1} d_{p,n}|e_p|+|\eta_0|,\quad n=1,2,\ldots,r.
$$

Then

$$
|e_r|\le C|\eta_0|,\quad r=1,2,\ldots,
$$

where C *is a positive constant free from* r *and* h.

Theorem 6. *The given ABM scheme* (30)–(31) *is conditionally stable.*

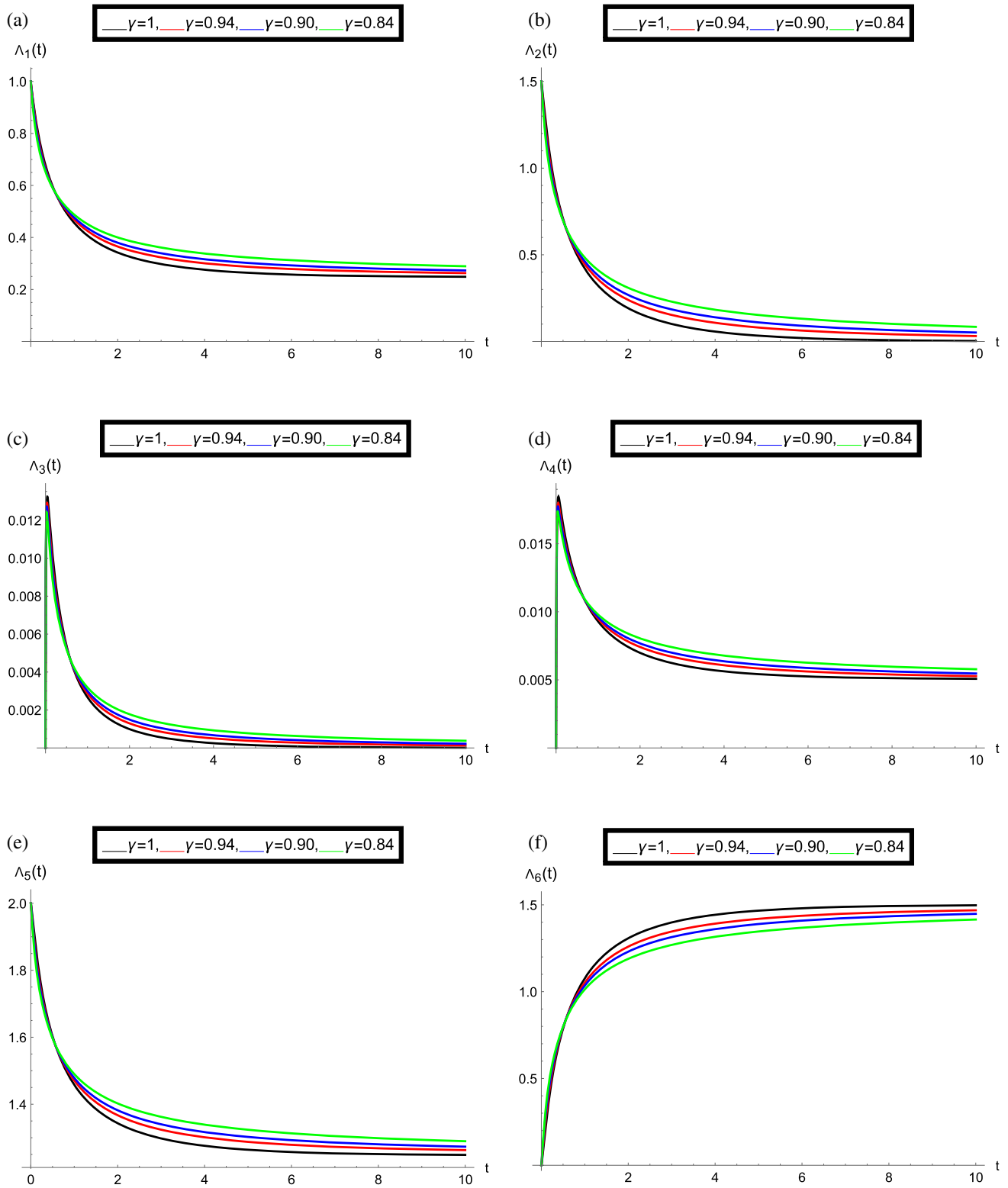

Figure 2. System dynamics for Set 1 at various fractional orders γ. (**a**) Variations in the constituent Λ_1 vs. time t, (**b**) variations in the constituent Λ_2 vs. time t, (**c**) variations in the constituent Λ_3 vs. time t, (**d**) variations in the constituent Λ_4 vs. time t, (**e**) variations in the constituent Λ_5 vs. time t and (**f**) variations in the constituent Λ_6 vs. time t.

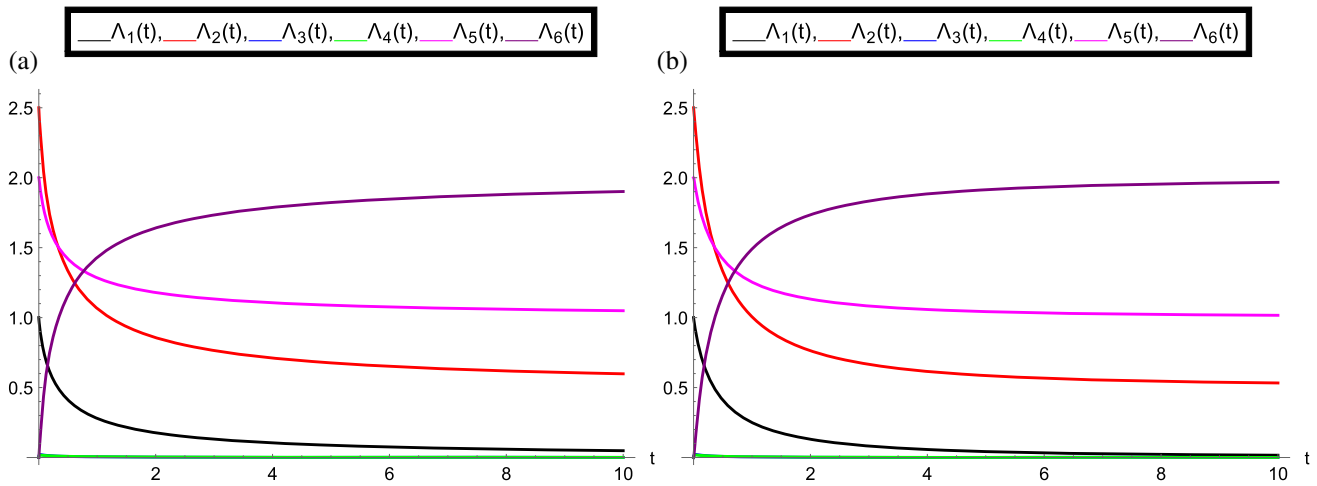

Figure 3. Constituents dynamics for Set 1 at some specific fractional orders. (**a**) Variations in the proposed constituents at fractional-order $\gamma = 0.85$ vs. time t and (**b**) variations in the proposed constituents at fractional-order $\gamma = 0.95$ vs. time t.

Proof. Let $\tilde{\Lambda}_{1_0}$, $\tilde{\Lambda}_{1_j}$ $(j = 0, \ldots, n+1)$ and $\tilde{\Lambda}_1^{P_{n+1}}$ $(n = 0, \ldots, N-1)$ be perturbations of Λ_{1_0}, Λ_{1_j} and $\Lambda_{1_{n+1}}^P$, respectively. Then, the following perturbations are derived by using eqs (30) and (31)

$$\begin{aligned}\tilde{\Lambda}_1^{P_{n+1}} &= \tilde{\Lambda}_{1_0} + \frac{1}{\Gamma(\gamma)} \\ &\quad \times \sum_{j=0}^{n} b_{j,n+1}\big(\mathcal{K}_1(t_j, \Lambda_{1_j} + \tilde{\Lambda}_{1_j}) \\ &\quad - \mathcal{K}_1(t_j, \Lambda_{1_j})\big), \end{aligned} \tag{32}$$

$$\begin{aligned}\tilde{\Lambda}_{1_{n+1}} &= \tilde{\Lambda}_{1_0} + \frac{h^\gamma}{\Gamma(\gamma+2)}\big(\mathcal{K}_1\big(t_{n+1}, \Lambda_{1_{n+1}}^P + \tilde{\Lambda}_{1_{n+1}}^P\big) \\ &\quad - \mathcal{K}_1\big(t_{n+1}, \Lambda_{1_{n+1}}^P\big)\big) \\ &\quad + \frac{h^\gamma}{\Gamma(\gamma+2)} \sum_{j=0}^{n} a_{j,n+1}\big(\mathcal{K}_1\big(t_j, \Lambda_{1_j} + \tilde{\Lambda}_{1_j}\big) \\ &\quad - \mathcal{K}_1\big(t_j, \Lambda_{1_j}\big)\big). \end{aligned} \tag{33}$$

Using the Lipschitz condition, we obtain

$$\begin{aligned}|\tilde{\Lambda}_{1_{n+1}}| &\le \zeta_0 + \frac{h^\gamma M}{\Gamma(\gamma+2)} \\ &\quad \times \left(|\tilde{\Lambda}_1^{P_{n+1}}| + \sum_{j=1}^{n} a_{j,n+1}|\tilde{\Lambda}_{1_j}|\right), \end{aligned} \tag{34}$$

where

$$\zeta_0 = \max_{0\le n\le N}\left\{|\tilde{\Lambda}_{1_0}| + \frac{h^\gamma M a_{n,0}}{\Gamma(\gamma+2)}|\tilde{\Lambda}_{1_0}|\right\}.$$

Also, from eq. (3.18) in [44] we get

$$|\tilde{\Lambda}_1^{P_{n+1}}| \le \eta_0 + \frac{M}{\Gamma(\gamma)} \sum_{j=1}^{n} b_{j,n+1}|\tilde{\Lambda}_{1_j}|, \tag{35}$$

where

$$\eta_0 = \max_{0\le n\le N}\left\{|\tilde{\Lambda}_{1_0}| + \frac{M b_{n,0}}{\Gamma(\gamma)}|\tilde{\Lambda}_{1_0}|\right\}.$$

Substituting $|\tilde{\Lambda}_1^{P_{n+1}}|$ from eq. (35) into eq. (34) results

$$\begin{aligned}|\tilde{\Lambda}_{1_{n+1}}| &\le \gamma_0 + \frac{h^\gamma M}{\Gamma(\gamma+2)}\left(\frac{M}{\Gamma(\gamma)} \sum_{j=1}^{n} b_{j,n+1}|\tilde{\Lambda}_{1_j}|\right. \\ &\quad \left. + \sum_{j=1}^{n} a_{j,n+1}|\tilde{\Lambda}_{1_j}|\right) \\ &\le \gamma_0 + \frac{h^\gamma M}{\Gamma(\gamma+2)} \\ &\quad \times \sum_{j=1}^{n}\left(\frac{M}{\Gamma(\gamma)} b_{j,n+1} + a_{j,n+1}\right)|\tilde{\Lambda}_{1_j}| \\ &\le \gamma_0 + \frac{h^\gamma M C_{\gamma,2}}{\Gamma(\gamma+2)} \sum_{j=1}^{n}(n+1-j)^{\gamma-1}|\tilde{\Lambda}_{1_j}|, \end{aligned} \tag{36}$$

where

$$\gamma_0 = \max\left\{\zeta_0 + \frac{h^\gamma M a_{n+1,n+1}}{\Gamma(\gamma+2)}\eta_0\right\}.$$

$C_{\gamma,2}$ is a positive constant only dependent on γ (Lemma 3) and h is taken to be small enough. Utilising Lemma 4, we get $|\tilde{\Lambda}_{1_{n+1}}| \le C\gamma_0$. This completes the proof.

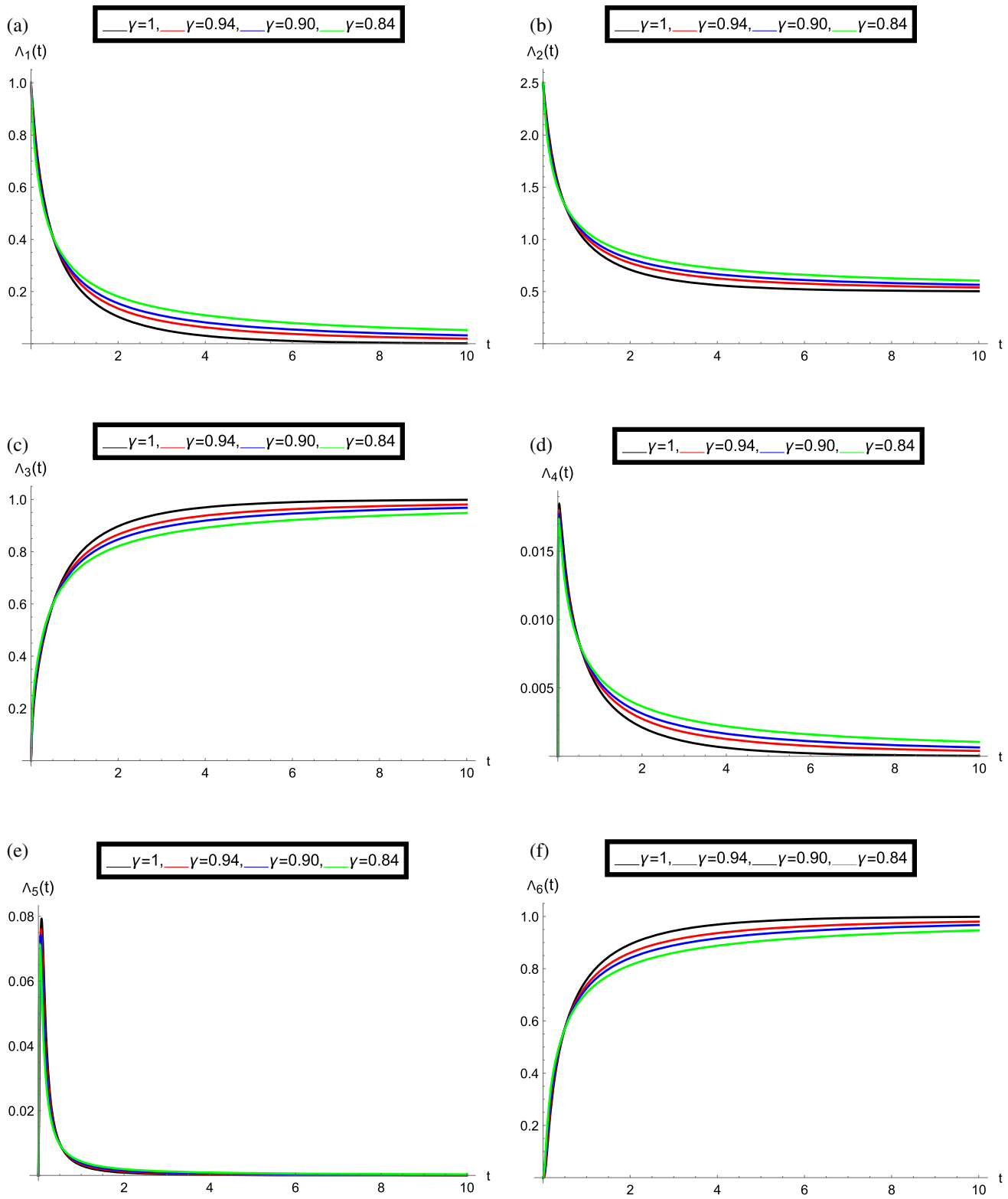

Figure 4. System dynamics for Set 2 at various fractional orders γ. (**a**) Variations in the constituent Λ_1 vs. time t, (**b**) variations in the constituent Λ_2 vs. time t, (**c**) variations in the constituent Λ_3 vs. time t, (**d**) variations in the constituent Λ_4 vs. time t, (**e**) variations in the constituent Λ_5 vs. time t and (**f**) variations in the constituent Λ_6 vs. time t.

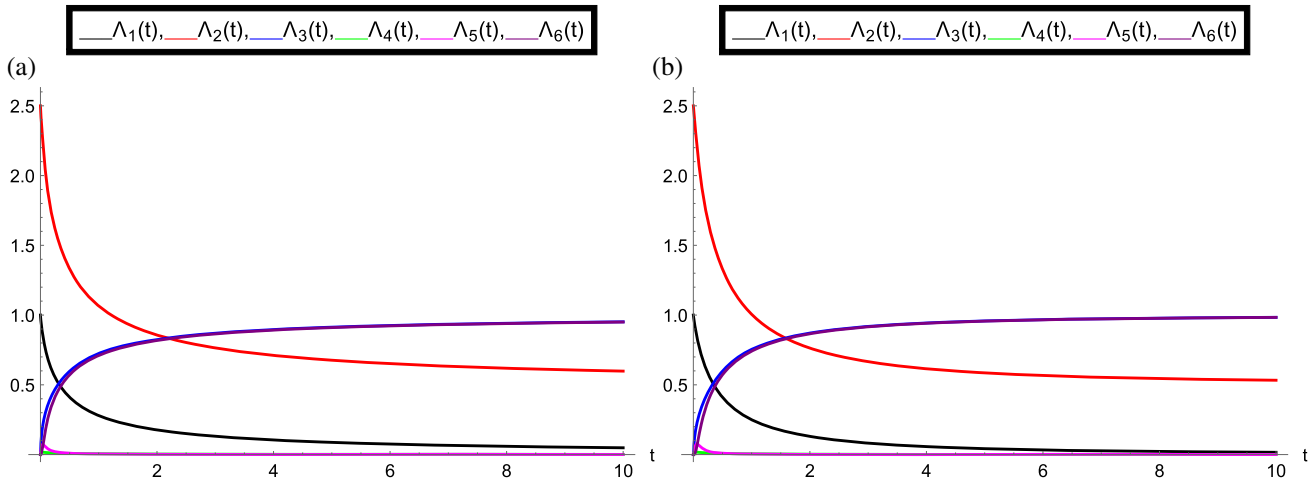

Figure 5. Constituent dynamics for Set 2 at some specific fractional orders. (**a**) Variations in the proposed constituents at fractional-order $\gamma = 0.85$ vs. time t and (**b**) variations in the proposed constituents at fractional-order $\gamma = 0.95$ vs. time t.

Table 1. Numerical outputs for Set 1 when fractional-order $\gamma = 0.85$.

t	Λ_1	Λ_2	Λ_3	Λ_4	Λ_5	Λ_6
0	1	2.5	0	0	2	0
1	0.279911	1.065475	0.004692	0.005654	1.284603	1.429832
2	0.176723	0.857011	0.002591	0.003565	1.179313	1.640399
3	0.130919	0.764477	0.001780	0.002639	1.132699	1.733743
4	0.104555	0.711216	0.001354	0.002106	1.105909	1.787430
5	0.087297	0.676352	0.001091	0.001757	1.088388	1.822557
6	0.075081	0.651672	0.000914	0.001511	1.075995	1.847414
7	0.065962	0.633251	0.000787	0.001327	1.066749	1.865962
8	0.058888	0.618959	0.000691	0.001184	1.059579	1.880350
9	0.053236	0.607541	0.000616	0.001070	1.053852	1.891842
10	0.048614	0.598205	0.000557	0.000977	1.049170	1.901239

Table 2. Numerical outputs for Set 1 at fractional-order $\gamma = 0.95$.

t	Λ_1	Λ_2	Λ_3	Λ_4	Λ_5	Λ_6
0	1	2.5	0	0	2	0
1	0.250393	1.005877	0.004084	0.005091	1.254477	1.490039
2	0.130307	0.763260	0.001782	0.002646	1.132089	1.734958
3	0.082087	0.665839	0.001021	0.001664	1.083109	1.833140
4	0.057080	0.615316	0.000671	0.001156	1.057751	1.884013
5	0.042331	0.585519	0.000480	0.000856	1.042811	1.914001
6	0.032908	0.566481	0.000364	0.000665	1.033272	1.933155
7	0.026537	0.553610	0.000288	0.000536	1.026826	1.946101
8	0.022038	0.544520	0.000236	0.000444	1.022274	1.955243
9	0.018745	0.537867	0.000199	0.000378	1.018944	1.961934
10	0.016260	0.532848	0.000171	0.000327	1.016432	1.966981

Table 3. Numerical outputs for Set 2 at fractional-order $\gamma = 0.85$.

t	Λ_1	Λ_2	Λ_3	Λ_4	Λ_5	Λ_6
0	1	2.5	0	0	0	0
1	0.279911	1.065475	0.724331	0.005654	0.004242	0.710194
2	0.176723	0.857011	0.825149	0.003565	0.001871	0.817841
3	0.130919	0.764477	0.870249	0.002639	0.001168	0.865274
4	0.104555	0.711216	0.896285	0.002106	0.000840	0.892499
5	0.087297	0.676352	0.913357	0.001757	0.000654	0.910292
6	0.075081	0.651672	0.925453	0.001511	0.000534	0.922875
7	0.065962	0.633251	0.934489	0.001327	0.000451	0.932260
8	0.058888	0.618959	0.941503	0.001184	0.000390	0.939538
9	0.053236	0.607541	0.947108	0.001070	0.000344	0.945350
10	0.048614	0.598205	0.951694	0.000977	0.000308	0.950102

Table 4. Numerical outputs for Set 2 at fractional-order $\gamma = 0.95$.

t	Λ_1	Λ_2	Λ_3	Λ_4	Λ_5	Λ_6
0	1	2.5	0	0	0	0
1	0.250393	1.005877	0.753086	0.005091	0.003480	0.741037
2	0.130307	0.763260	0.870866	0.002646	0.001173	0.865874
3	0.082087	0.665899	0.918521	0.001664	0.000608	0.915640
4	0.057080	0.615316	0.943299	0.001156	0.000379	0.941384
5	0.042331	0.585519	0.957932	0.000856	0.000263	0.956549
6	0.032908	0.566481	0.967287	0.000665	0.000196	0.966231
7	0.026537	0.553610	0.973616	0.000536	0.000153	0.972774
8	0.022038	0.544520	0.978086	0.000444	0.000124	0.977393
9	0.018745	0.537867	0.981359	0.000378	0.000104	0.980774
10	0.016260	0.532848	0.983829	0.000327	0.000089	0.983323

5. Experimental observations

In this section, we explore the model dynamics with the help of some graphical representations by using *Mathematica* software. We use the values of the reaction rates $\beta_1 = 1,\ \beta_2 = 50,\ \beta_3 = 100$ as given in ref. [6] with brief explanation.

As we know that the molar concentration must be non-negative, constituents $\Lambda_1,\ \Lambda_2,\ \Lambda_3,\ \Lambda_4,\ \Lambda_5$ and Λ_6 are taken non-negative. Also, $\Lambda_1(0)$ and $\Lambda_2(0)$ must be non-zero for an alkali–silica reaction to exist. It should be remembered that $\Lambda_5(0)$ will have both the generated water (eq. (6)) and the primary level of water $\Lambda_5(0) \geq 0$. For simplicity, we fixed $\Lambda_3(0),\ \Lambda_4(0),\ \Lambda_6(0) = 0$. Also it is generally taken that the ASR is defined by the finite silica (i.e. $\Lambda_2(0) \geq \Lambda_1(0)$), the condition when $\Lambda_2(0) \leq \Lambda_1(0)$ will also be taken.

When $\Lambda_2(0) \geq 2\Lambda_1(0)$, figures 2 and 3 are plotted for $\Lambda_1 = 1,\ \Lambda_2 = 2.5,\ \Lambda_3 = 0,\ \Lambda_4 = 0,\ \Lambda_5 = 2,\ \Lambda_6 = 0$ (Set 1). In figure 2, all the given constituents at various fractional-order values $\gamma = 1,\ 0.94,\ 0.90,\ 0.84$ vs. time t are plotted, separately. Here we notice, when the time range increases then the amount of siloxane Λ_1 swiftly decreases and tends to zero, hydroxyl ions Λ_2 decreases and after some time tends to approximately around 0.6, alkali-silicate gel amount Λ_3 goes down very swiftly and tends to zero, silicic acid Λ_4 also goes down very sharply and tends to zero, water quantity Λ_5 decreases, and expanded alkali silicate (gel) Λ_6 increases sharply. In figure 3, all the classes are plotted together for fractional-orders $\gamma = 0.85$ (figure 3a) and $\gamma = 0.95$ (figure 3b) vs. time t for understanding the variations in the given quantities with respect to each other.

For the same case $\Lambda_2(0) \geq 2\Lambda_1(0)$, figures 4 are 5 are plotted for $\Lambda_1 = 1,\ \Lambda_2 = 2.5,\ \Lambda_3 = 0,\ \Lambda_4 = 0,\ \Lambda_5 = 0,\ \Lambda_6 = 0$ (Set 2). In figure 4, all the given constituents at various fractional-order values $\gamma = 1,\ 0.94,\ 0.90,\ 0.84$ vs. time t are plotted, separately. Here we can observe that the variations in the water quantity Λ_5 are much sharper than Set 1 because of the changes in the initial value of Λ_5. In figure 5, all classes are plotted together for fractional orders $\gamma = 0.85$ (figure 5a) and $\gamma = 0.95$ (figure 5b) vs. time t. Numerical outputs for Sets 1 and 2 when $\gamma = 0.85$ and $\gamma = 0.95$ are given in tables 1–4, respectively.

Now, when $\Lambda_2(0) < 2\Lambda_1(0)$, figures 6 and 7 are given for $\Lambda_1 = 1,\ \Lambda_2 = 1.5,\ \Lambda_3 = 0,\ \Lambda_4 =$

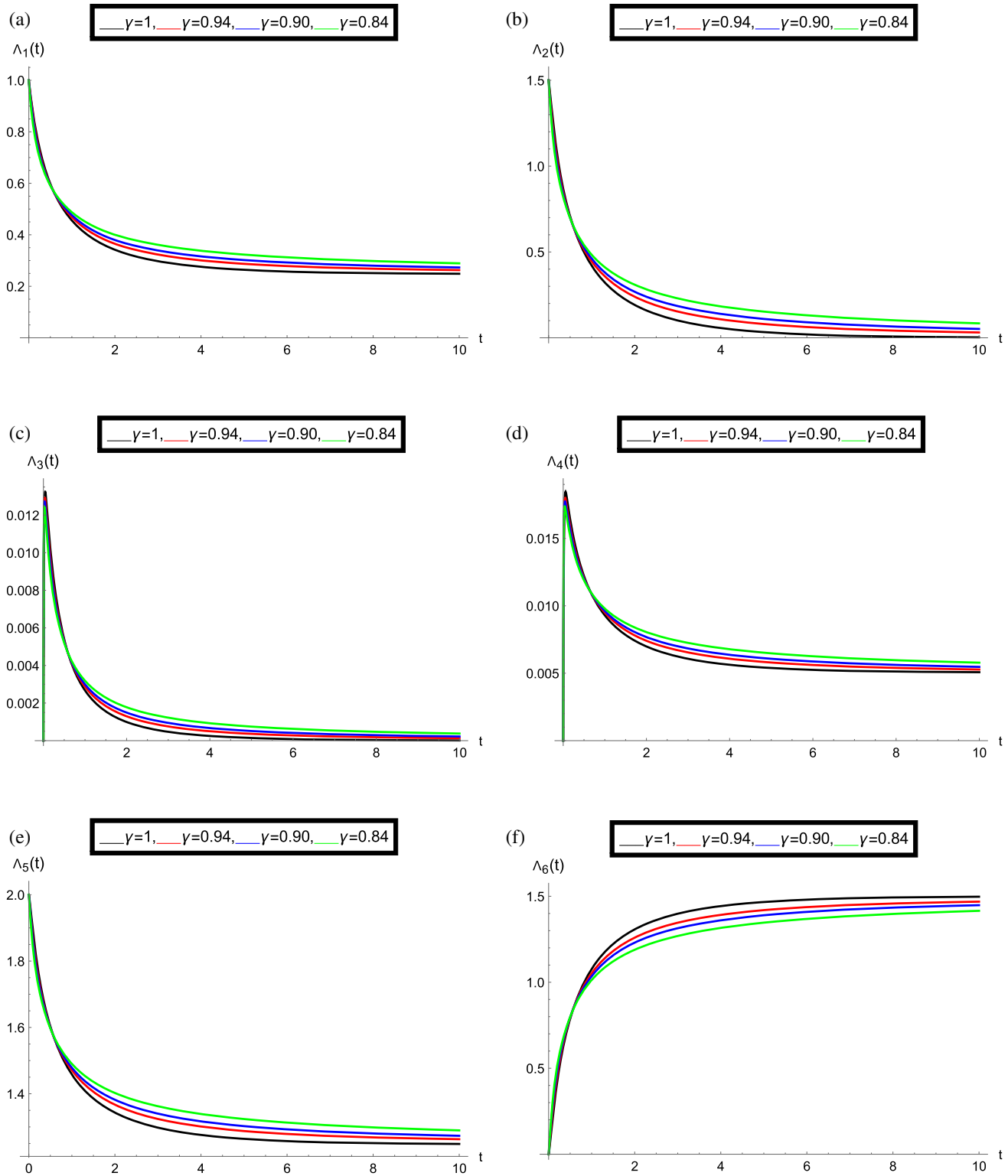

Figure 6. System dynamics for Set 3 at various fractional orders γ. (**a**) variations in the constituent Λ_1 vs. time t, (**b**) variations in the constituent Λ_2 vs. time t, (**c**) variations in the constituent Λ_3 vs. time t, (**d**) variations in the constituent Λ_4 vs. time t, (**e**) variations in the constituent Λ_5 vs. time t and (**f**) variations in the constituent Λ_6 vs. time t.

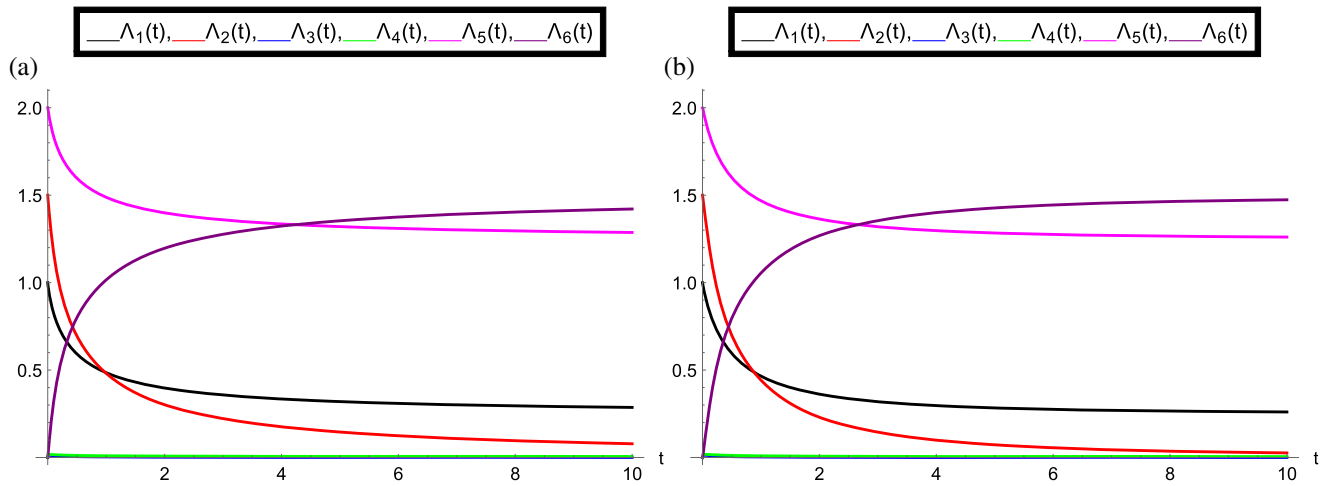

Figure 7. Constituent dynamic for Set 3 at some specific fractional orders. (**a**) Variations in the proposed constituents at fractional-order $\gamma = 0.85$ vs. time t and **(b)** variations in the proposed constituents at fractional-order $\gamma = 0.95$ vs. time t.

0, $\Lambda_5 = 2$, $\Lambda_6 = 0$ (Set 3). In figure 6, all the given constituents at various fractional-order values $\gamma = 1,\ 0.94,\ 0.90,\ 0.84$ vs. time t are plotted, separately. Here, when the time range increases then the amount of siloxane Λ_1 decreases but does not tend to zero, hydroxyl ions Λ_2 decreases and after some time tends to approximately zero, alkali-silicate gel Λ_3 decreases very sharply and tends to zero, silicic acid Λ_4 also decreases but does not tend to zero, water quantity Λ_5 decreases, and expanded alkali silicate (gel) Λ_6 increases sharply. In the collection of figure 7, all classes are plotted together for fractional-order values $\gamma = 0.85$ (figure 7a) and $\gamma = 0.95$ (figure 7b) vs. time t.

For the same case $\Lambda_2(0) \geq 2\Lambda_1(0)$, figures 8 and 9 are plotted for $\Lambda_1 = 1$, $\Lambda_2 = 1.5$, $\Lambda_3 = 0$, $\Lambda_4 = 0$, $\Lambda_5 = 0$, $\Lambda_6 = 0$ (Set 4). In figure 8, all the given constituents at various fractional-order values $\gamma = 1,\ 0.94,\ 0.90,\ 0.84$ vs. time t are plotted, separately. In figure 9, all classes are plotted together for fractional orders $\gamma = 0.85$ (figure 9a) and $\gamma = 0.95$ (figure 9b) vs. time t. Numerical outputs for Sets 3 and 4 at $\gamma = 0.85$ and $\gamma = 0.95$ are given in tables 5–8, respectively.

From the above observations, we notice that Λ_6 is abundant when the amount of water is more in the model and the starting alkali concentration is abundant. That means Λ_6 is big when $\Lambda_5(0)$ and $\Lambda_2(0)$ are expanded. That is exactly what we know about ASR, that a least proportional moisture of around 80% is demanded for the reaction to be quantifiable. In the above simulations, we used two different values of Λ_5 to show the role of the initial values of water concentration in the production of gel. It is estimated that the proportional initial values of the concentrations of silica, alkali and water in the model headship to four distinct possibilities of the estimations of ultimate alkali silicate gel concentration. When the amount of alkali is less than silica, a smaller amount of the propagated gel is yielded. This study specifies that the outputs are comparatively robust in terms of the preference of opted rates of reaction for each value of fractional-order γ. The given numerical method in the form of Caputo fractional derivative works well to understand the given chemical reaction dynamics.

6. Conclusion

In this research, a non-linear fractional-order mathematical model to study the dynamics of alkali–silica chemical reaction by using Caputo derivative has been analysed. We have proved the existence of a unique solution by using some novel properties of Mittag–Leffler function along with fixed point theory. Stability of the proposed system was also proved by using Ulam–Hyers methodology. For deriving the fractional-order numerical solution, we have used a reliable numerical method called Adams–Bashforth–Moulton scheme. The stability of the given method has also been proven. Many graphs are plotted to understand the role of concentrations of the given constituents in the ASR. The main motivation to use Caputo fractional derivative in the given model was to solve the ASR dynamics much more effectively with the novel features of fractional derivatives because in terms of memory effects, these derivative operators are much better than the integer-order derivatives. This study strongly justifies the role of fractional derivatives in chemical reactions.

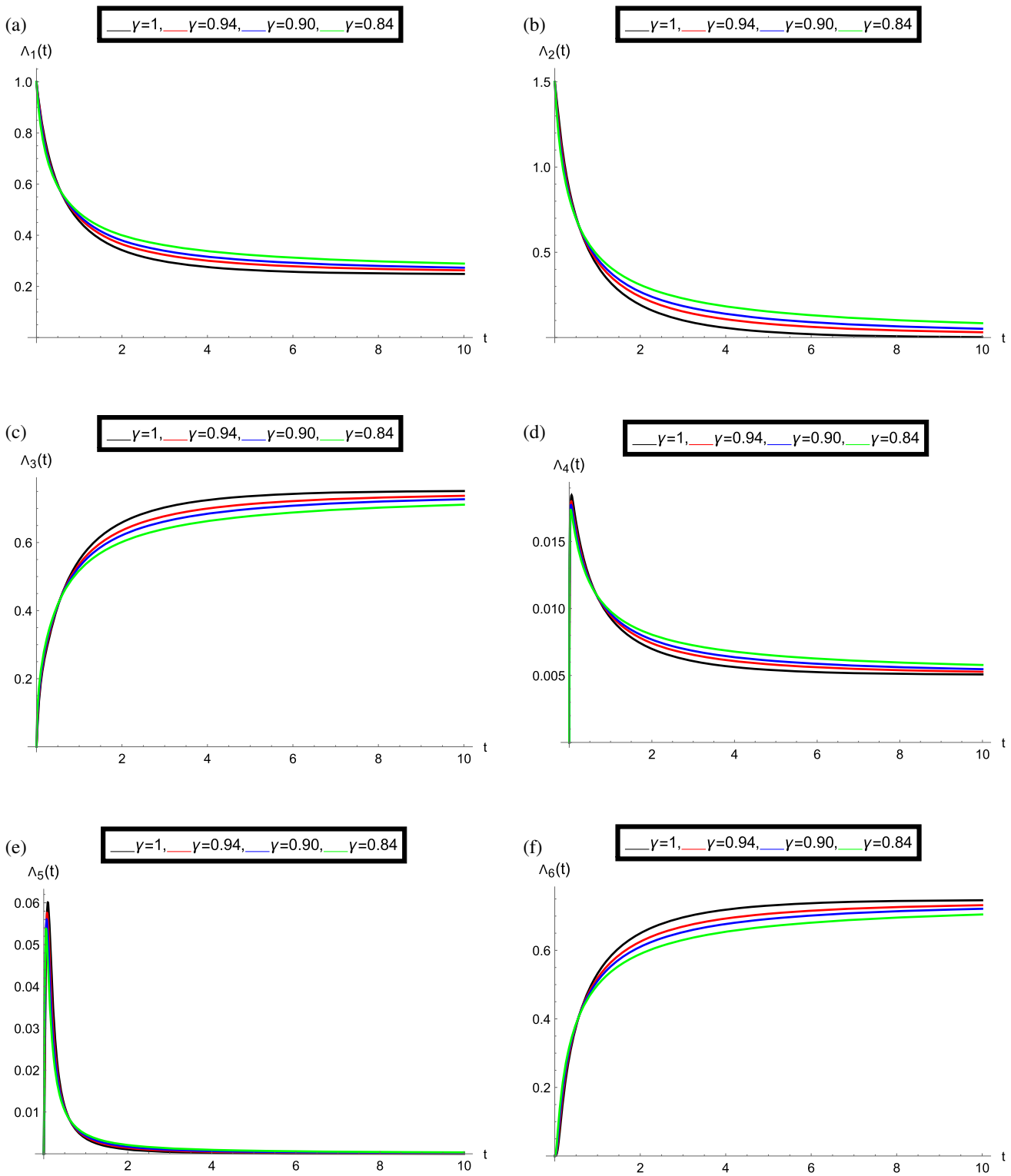

Figure 8. System dynamics for Set 4 at various fractional orders γ. (**a**) Variations in the constituent Λ_1 vs. time t, (**b**) variations in the constituent Λ_2 vs. time t, (**c**) variations in the constituent Λ_3 vs. time t, (**d**) variations in the constituent Λ_4 vs. time t, (**e**) variations in the constituent Λ_5 vs. time t and (**f**) variations in the constituent Λ_6 vs. time t.

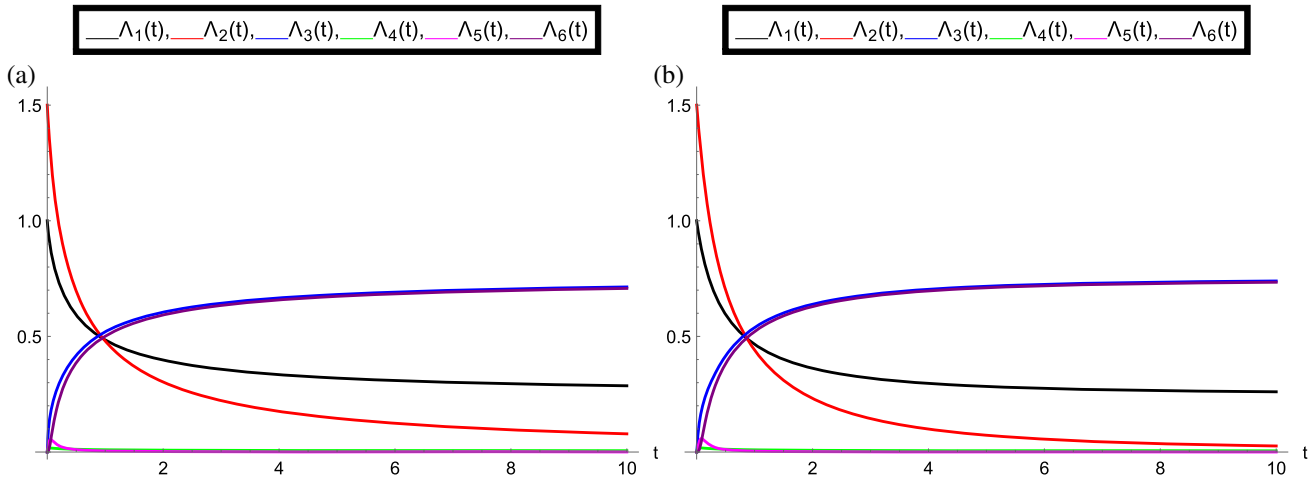

Figure 9. Constituent dynamics for Set 4 at some specific fractional orders. (**a**) Variations in the proposed constituents at fractional-order $\gamma = 0.85$ vs. time t and (**b**) variations in the proposed constituents at fractional-order $\gamma = 0.95$ vs. time t.

Table 5. Numerical outputs for Set 3 at fractional-order $\gamma = 0.85$.

t	Λ_1	Λ_2	Λ_3	Λ_4	Λ_5	Λ_6
0	1	1.5	0	0	2	0
1	0.485125	0.480015	0.003155	0.009765	1.488280	1.016830
2	0.397331	0.302652	0.001730	0.007990	1.399061	1.195618
3	0.357556	0.222295	0.001176	0.007182	1.358732	1.276529
4	0.334587	0.175888	0.000885	0.006715	1.335472	1.323227
5	0.319588	0.145585	0.000707	0.006409	1.320296	1.353707
6	0.309024	0.124240	0.000588	0.006193	1.309612	1.375172
7	0.301185	0.108402	0.000503	0.006032	1.301688	1.391095
8	0.295142	0.096191	0.000439	0.005908	1.295581	1.403369
9	0.290344	0.086497	0.000390	0.005809	1.290734	1.413113
10	0.286444	0.078617	0.000351	0.005729	1.286795	1.421032

Table 6. Numerical outputs for Set 3 at fractional-order $\gamma = 0.95$.

t	Λ_1	Λ_2	Λ_3	Λ_4	Λ_5	Λ_6
0	1	1.5	0	0	2	0
1	0.465639	0.440734	0.002837	0.009456	1.468476	1.056430
2	0.362150	0.231646	0.001246	0.007345	1.363396	1.267108
3	0.319170	0.144804	0.000708	0.006464	1.319878	1.354489
4	0.296674	0.099348	0.000459	0.006000	1.297132	1.400194
5	0.283416	0.072557	0.000323	0.005724	1.283739	1.427120
6	0.274999	0.055544	0.000241	0.005546	1.275240	1.444215
7	0.269362	0.044149	0.000188	0.005426	1.269550	1.455662
8	0.265426	0.036193	0.000153	0.005340	1.265579	1.463655
9	0.262581	0.030440	0.000127	0.005277	1.262709	1.469433
10	0.260463	0.026155	0.000108	0.005230	1.260571	1.473736

Table 7. Numerical outputs for Set 4 at fractional-order $\gamma = 0.85$.

t	Λ_1	Λ_2	Λ_3	Λ_4	Λ_5	Λ_6
0	1	1.5	0	0	0	0
1	0.485125	0.480015	0.519508	0.009765	0.004633	0.500477
2	0.397331	0.302652	0.604697	0.007990	0.002029	0.592651
3	0.357556	0.222295	0.643697	0.007182	0.001253	0.634009
4	0.334587	0.175888	0.666307	0.006715	0.000893	0.657805
5	0.319588	0.145585	0.681101	0.006409	0.000690	0.673313
6	0.309024	0.124240	0.691536	0.006193	0.000559	0.694224
7	0.301185	0.108402	0.699285	0.006032	0.000470	0.692313
8	0.295142	0.096191	0.705263	0.005908	0.000405	0.698546
9	0.290344	0.086497	0.710012	0.005809	0.000355	0.703492
10	0.286444	0.078617	0.713873	0.005729	0.000317	0.707510

Table 8. Numerical outputs for Set 4 at fractional-order $\gamma = 0.95$.

t	Λ_1	Λ_2	Λ_3	Λ_4	Λ_5	Λ_6
0	1	1.5	0	0	0	0
1	0.465639	0.440734	0.538355	0.009456	0.003994	0.520911
2	0.362150	0.231646	0.639202	0.007345	0.001352	0.629152
3	0.319170	0.144804	0.681525	0.006464	0.000694	0.673672
4	0.296674	0.099348	0.703753	0.006000	0.000427	0.696899
5	0.283416	0.072557	0.716875	0.005724	0.000292	0.710568
6	0.274999	0.055544	0.725215	0.005546	0.000214	0.719241
7	0.269362	0.044149	0.730803	0.005426	0.000165	0.725048
8	0.265426	0.036193	0.734706	0.005340	0.000132	0.729101
9	0.262581	0.030440	0.737528	0.005277	0.000109	0.732032
10	0.260463	0.026155	0.739630	0.005230	0.000093	0.734215

In future, such reactions can be modelled by other fractional derivatives like Caputo–Fabrizio, Katugampola, Atangana–Baleanu etc.

Acknowledgements

The authors would like to thank Taif University for its financial grant, via Taif University Researchers Supporting Project number (TURSP-2020/91), Taif University, Taif, Saudi Arabia.

References

[1] T E Stanton, *Trans. Am. Soc. Civ. Eng.* **107**, 54 (1942)
[2] T Ichikawa and M Miura, *Cem. Concr. Res.* **37**, 1291 (2007)
[3] S Chatterji, *Cem. Concr. Compos.* **27**, 788 (2005)
[4] R Dron and F Brivot, *Cem. Concr. Res.* **22**, 941 (1992)
[5] T Katayama, *Proceedings of the 14th International Conference on Alkali-aggregate Reaction* (Austin, Texas, USA, 2012)
[6] V E Saouma, R A Martin, M A Hariri-Ardebili and T Katayama, *Cem. Concr. Res.* **68**, 184 (2015)
[7] T Katayama, *Proceedings of the 13th International Conference on Alkali-aggregate Reaction* (Trondheim, Norway, 2008)
[8] T Katayama, *Proceedings of the 14th International Conference on Alkali-aggregate Reaction* (Austin, Texas, 2012) pp. 20–25
[9] A Kilbas, H M Srivastava and J J Trujillo, *Theory and applications of fractional differential equations* (Elsevier Science, New York, 2006)
[10] Z Hammouch, M Yavuz and N Ozdemir, *Math. Mod. Numer. Simul. Appl.* **1(1)**, 11 (2021)
[11] P Veeresha, M Yavuz and C Baishya, *Int. J. Opt. Cont. Theor. Appl.* **11(3)**, 52 (2021)
[12] P A Naik, Z Eskandari and H E Shahraki, *Math. Mod. Numer. Simul. Appl.* **1(2)**, 95 (2021)
[13] P Kumar, V S Erturk, R Banerjee, M Yavuz and V Govindaraj, *Phys. Scr.* **96(12)**, 124044 (2021)
[14] R Ikram, A Khan, M Zahri, A Saeed, M Yavuz and P Kumam, *Comput. Biol. Med.* **141**, 105115 (2022)
[15] H Joshi and B K Jha, *Math. Mod. Numer. Simul. Appl.* **1(2)**, 84 (2021)
[16] F Ozkose, S Yılmaz, M Yavuz, I Ozturk, M T Şenel, B S Bagcı, M Dogan and O Onal, *Eur. Phys. J. Plus* **137(1)**, 1 (2022)

[17] F Ozkose and M Yavuz, *Comput. Biol. Med.* 105044 (2021)
[18] V S Erturk and P Kumar, *Chaos Solitons Fractals* **139**, 110280 (2021)
[19] W Gao, P Veeresha, H M Baskonus, D G Prakasha and P Kumar, *Chaos Solitons Fractals* **138**, 109929 (2020)
[20] P Kumar, V S Erturk, A Yusuf and S Kumar, *Chaos Solitons Fractals* **150**, 111123 (2021)
[21] P Kumar, V S Erturk and M Murillo-Arcila, *Chaos Solitons Fractals* **150**, 111091 (2021)
[22] P Kumar, V S Erturk, M Murillo-Arcila, R Banerjee and A Manickam, *Adv. Differ. Equ.* **2021**, 1 (2021).
[23] K N Nabi, H Abboubakar and P Kumar, *Chaos Solitons Fractals* **141**, 110283 (2020)
[24] P Kumar and V S Erturk, *Chaos Solitons Fractals* **144**, 110672 (2021)
[25] H Abboubakar, P Kumar, V S Erturk and A Kumar, *Int. J. Mod. Simul. Sci. Comput.* **12**, 2150037(2021)
[26] P Kumar, V S Erturk, K S Nisar, W Jamshed and M S Mohamed, *Alex. Eng. J.* special issue paper (2021)
[27] K N Nabi, P Kumar and V S Erturk, *Chaos Solitons Fractals* **145**, 110689 (2021)
[28] H Abboubakar, P Kumar, N A Rangaig and S Kumar, *Int. J. Mod. Simul. Sci. Comput.* **12**, 2150013 (2020)
[29] P Kumar and V S Erturk, *Math. Meth. Appl. Sci.* special issue paper, 1-14 (2021)
[30] P Kumar, V S Erturk and M Murillo-Arcila, *Res. Phys.* **24**, 104213 (2021)
[31] P Kumar, V S Erturk, A Yusuf and T A Sulaiman, *Int. J. Model. Simul. Sci. Comput.* **12**, 2150055 (2021)
[32] P Kumar, V S Erturk, A Yusuf, K S Nisar and S F Abdelwahab, *Res. Phys.* **25**, 104281 (2021)
[33] P Kumar, V S Erturk and K S Nisar, *Math. Methods Appl. Sci.* **44**, 11404 (2021)
[34] P Kumar, V S Erturk and H Almusawa, *Res. Phys.* **24**, 104186 (2021)
[35] P Kumar, V S Erturk and A Kumar, *J. Math. Ext.* **15** (2021)
[36] Z Odibat, V S Erturk, P Kumar and V Govindaraj, *Phys. Scr.* **96**, 125213 (2021)
[37] Z Odibat and D Baleanu, *Appl. Numer. Math.* **156**, 94 (2020)
[38] C N Angstmann, B A Jacobs, B I Henry and Z Xu, *Mathematics* **8**, 2023 (2020)
[39] I Podlubny, *Fractional differential equations* (Academic Press, San Diego, 1998)
[40] C S Sin and L Zheng, *Fract. Calc. Appl. Anal.* **19**, 765 (2016)
[41] K Diethelm, *The analysis of fractional differential equations* (Springer Science & Business Media, New York, 2010)
[42] H J Haubold, A M Mathai and R K Saxena, *J. Appl. Math.* **2011** (2011)
[43] A Ben Makhlouf and E S El-Hady, *Math. Probl. Eng.* **2021** (2021)
[44] C Li and F Zeng, *Numer. Funct. Anal. Opt.* **34**, 149 (2013)